Dayside flow bursts in the Earth's outer magnetosphere

S.-H. Chen
Universities Space Research Association, Seabrook, Maryland, USA

T. E. Moore
Interplanetary Physics Branch, NASA Goddard Space Flight Center, Greenbelt, Maryland, USA

Received 25 April 2003; revised 16 January 2004; accepted 5 February 2004; published 20 March 2004.

[1] Observations from the Polar/Thermal Ion Dynamics Experiment indicate the presence of cold magnetospheric/ionospheric H^+, He^+, and a trace of O^+ in the vicinity of the subsolar magnetopause during intervals of moderate geomagnetic activity ($Kp \sim 4$). These cold ions were accelerated to a perpendicular speed ($\Delta V_{\perp B}$) of the order of 100 km s^{-1} or 0.3 M_A outward, relative to the magnetopause boundary oscillations. The accelerated flows produced $\sim$4 mV m^{-1} in convection electric field and carried $\sim$1–100 ions cm^{-3} in number density or $\sim 0.1-5 \times 10^8$ ions cm^{-2} s^{-1} in particle flux or $4 \times 10^{25}-2 \times 10^{27}$ ions s^{-1} in transfer rate (assuming sunward convecting flux tube with latitudinal cross-section of 1 R_E in width and 10 R_E in length along magnetopause). This rate of plasma transfer from inside the magnetopause is comparable with that entering the LLBL with the same incident cross section on the magnetopause from the solar wind influx. The occurrence of these flow burst events is accompanied by changes in the local magnetic field orientation, departing from nominal magnetospheric magnetic field, and is sensitive to the variation in the IMF clock angle. We suggest that the magnetospheric/ionospheric ions contribute plasma of dynamical significance to physical processes such as magnetic reconnection, for the cases presented in this study at the subsolar magnetopause. *INDEX TERMS:* 2784 Magnetospheric Physics: Solar wind/magnetosphere interactions; 2740 Magnetospheric Physics: Magnetospheric configuration and dynamics; 2724 Magnetospheric Physics: Magnetopause, cusp, and boundary layers; 2752 Magnetospheric Physics: MHD waves and instabilities; 2736 Magnetospheric Physics: Magnetosphere/ionosphere interactions; *KEYWORDS:* reconnection, magnetopause, solar wind-magnetosphere interaction, magnetosphere-ionosphere coupling, magnetic field line merging, plasma instabilities

Citation: Chen, S.-H., and T. E. Moore (2004), Dayside flow bursts in the Earth's outer magnetosphere, *J. Geophys. Res.*, *109*, A03215, doi:10.1029/2003JA010007.

1. Introduction

[2] Plasma in the Earth's magnetosphere has two major sources, the solar wind (heliogenic) and the ionosphere (geogenic). Solar wind plasma enters at the magnetopause when the magnetospheric magnetic field opens to the interplanetary magnetic field, forming the low-latitude boundary layer (LLBL) and high-latitude boundary layer (plasma mantle). Ionospheric plasma directly populates closed magnetic flux tubes and forms the plasmasphere or populates open magnetic flux tubes at the cusp/cleft creating ion fountains and reaches the LLBL either through the detachment of plasmasphere on closed field lines at low latitudes or along open field lines at high latitudes. Plasmas of both origins mix and evolve in the LLBL. Understanding their properties helps in characterizing the fundamental physical process of interaction between solar wind plasma and ionospheric plasma atmospheres.

[3] The highest density cold plasmas of ionospheric origin are confined within the inner magnetosphere or plasmasphere, extending to a distance within the geosynchronous orbit. However, the density of tenuous cold plasmas in the outer magnetosphere can be greatly enhanced to a similar level by the formation of plasmaspheric drainage plumes or detached regions [*Grebowsky*, 1970; *Chappell*, 1974]. These plasma plumes have been observed by many spacecraft such as Ogo 4, 5, and 6, Ariel 3, ATS, and LANL [*Taylor et al.* 1971; *Grebowsky et al.*, 1973; *Chappell*, 1974; *Maynard and Chen*, 1975; *Horwitz et al.*, 1990; *Moldwin et al.*, 1995; *Sandel et al.*, 2001]. The detached plasma extends over a wide range of local times and space between plasmapause and magnetopause and contributes to many physical processes from microscale to macroscale in the region, such as the production of ULF waves [*Barfield and McPherron*, 1972; *Singer et al.*, 1981; *Takahashi et al.*, 2002; *Engebretson et al.*, 2002], ELF waves [*Kivelson and Russell*, 1973], and consequently relativistic electrons [*Thorne*, 1974; *Summers and Thorne*, 2003], or indirectly the seeding of the substorms [*Brice*, 1970] and the plasma sheet in the tail of the magnetosphere [*Hill*, 1974; *Borovsky et al.*, 1997; *Elphic et al.*, 1997; *Seki et al.*, 2002]. Near the magnetopause, the last closed magnetic flux tubes convect sunward taking part in the global convection and bringing plasmaspheric

0148-0227/04/2003JA010007

Table 1. List of Flow Burst Events

Time, UT		Distance, R_E	MLT, hours	MLat, deg	Inv. Lat., deg	*AE*	*Dst*	*Kp*
20 March 2001	0200–0400	9.5	12.4	14.3	71.6	400–900	−87–−73	5^+
7 February 2002	2200–2400	9.5	14.4	18.2	71.0	100–500	−12–−7	3^+
17 February 2002	0430–0800	8.1	14.2	17.7	70.4	200–450	−2–+20	4^-
5 March 2002	0300–0700	9.0	13.0	9.2	70.7	200–700	−40–−25	4^-
2 April 2002	0730–1030	9.4	11.3	8.1	71.2	300–1000	−40–−30	4
14 May 2002	0600–0730	9.6	8.4	3.4	71.2	400–800	−57–−42	4

particles toward the magnetopause. In the magnetospheric boundary layer or LLBL, sources converge bringing ionospheric plasma to interact with solar wind plasma. Ambiguities emerge as to the paths radial convection or field-aligned ionospheric plasmas may take to the LLBL and which is the more crucial physical process.

[4] Ions with ionospheric signatures have been observed in LLBL by ISEE and AMPTE/CCE, which was interpreted as a result of direct injection from the ionosphere along the field line [*Fuselier et al.*, 1989; *Fuselier et al.*, 1991; *Fuselier*, 1995; *Fuselier et al.*, 1995]. When reconnections occur at the magnetopause, ions carried by the reconnected flux tubes once closed should contribute to the reconnection process and populate LLBL in a way similar to its counterpart at the magnetosheath side. Except during intervals of extreme geomagnetic activities when the magnetopause is pushed near the geosynchronous orbit [*Elphic et al.*, 1996; *Su et al.*, 2000; *Su et al.*, 2001], observations of these cold ions with distinguishable ionospheric composition (e.g., He^+ and O^+) convected from inside are rare (see, however, *Peterson et al.* [1982], *Gosling et al.* [1990], *Fuselier et al.* [1995], and *Sauvaud et al.* [2001]). This is due to instrument energy threshold and resolution attributes that were inadequate to measure ions with much narrower thermal spreading and smaller convection speed. It is the objective of this study to investigate qualitatively and quantitatively how the cold plasmaspheric ions contribute to physical processes in the LLBL from inside when the magnetopause is at its nominal position.

[5] While observations of ions in the LLBL at medium to high energy (hundreds of eV to 1 KeV) are ample (e.g., ISEE, AMPTE/IRM, AMPTE/CCE, GEOTAIL), observations of cold ions in the 1–100 eV range with adequate energy resolution are rare. We use data from the Thermal Ion Dynamics Experiment (TIDE) [*Moore et al.*, 1995] on Polar spacecraft during the years of 2001 and 2002, when its apogees were near the equatorial plane, to study the dynamics of cold ions with the energy range between the spacecraft potential of a few eV and 375 eV in dayside magnetopause boundary layers. TIDE is a time of flight instrument, so each particle gets detected as it enters a speed course (START) and as it leaves it (STOP). The time difference gives the velocity, which knowing the energy gives the mass (all per unit charge). TIDE has time resolution of ~6 s and energy resolution of >5% which provides good measurements of plasma moments for cold ions such as H^+, He^{+2}, He^+, N^+, O^{+2}, and O^+ that have relatively narrow thermal speeds, provided the peak energies of these ions falls in the energy range of the instrument. In this study, we only use STOPS component in TIDE data, which provides collapsed three-dimensional (3-D) measurements as 2-D velocity distributions in the spin plane, since the STARTS component, which provide three-dimensional mass-resolved (time of flight) measurements, was not available after late 1996. All the implications of the collapsing of the three-dimensional into two-dimensional measurement have been considered carefully while performing the analysis. With energy range encompassing both ionospheric and magnetosheath plasmas, and good energy and time resolutions, these measurements will add significantly to our already profound knowledge of plasmas in the dayside magnetospheric boundary layers. Initial results showing the presence of ionospheric cold plasmas at the magnetopause have been reported by *Chandler and Moore* [2003].

2. Observations and Analyses

[6] Combining the ion measurements from TIDE (STOPS), and magnetic field from the Magnetic Field Experiment (MFE) [*Russell et al.*, 1995] on the Polar spacecraft, with solar wind parameters from ACE, we

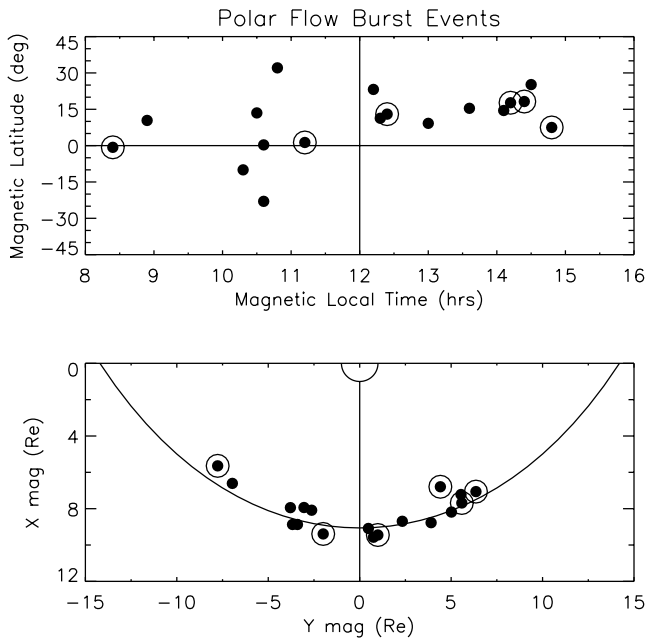

Figure 1. Positions of magnetopause crossings by Polar in our data set. The upper panel shows them in magnetic latitude versus magnetic local time. The lower panel shows them in the magnetic equator. The circled dots represent the events for which flow bursts were observed as listed in Table 1. The position of model magnetopause [*Shue et al.*, 1997] at solar wind dynamic pressure of 3 nPa and IMF $B_z = -5.0$ nT is shown.

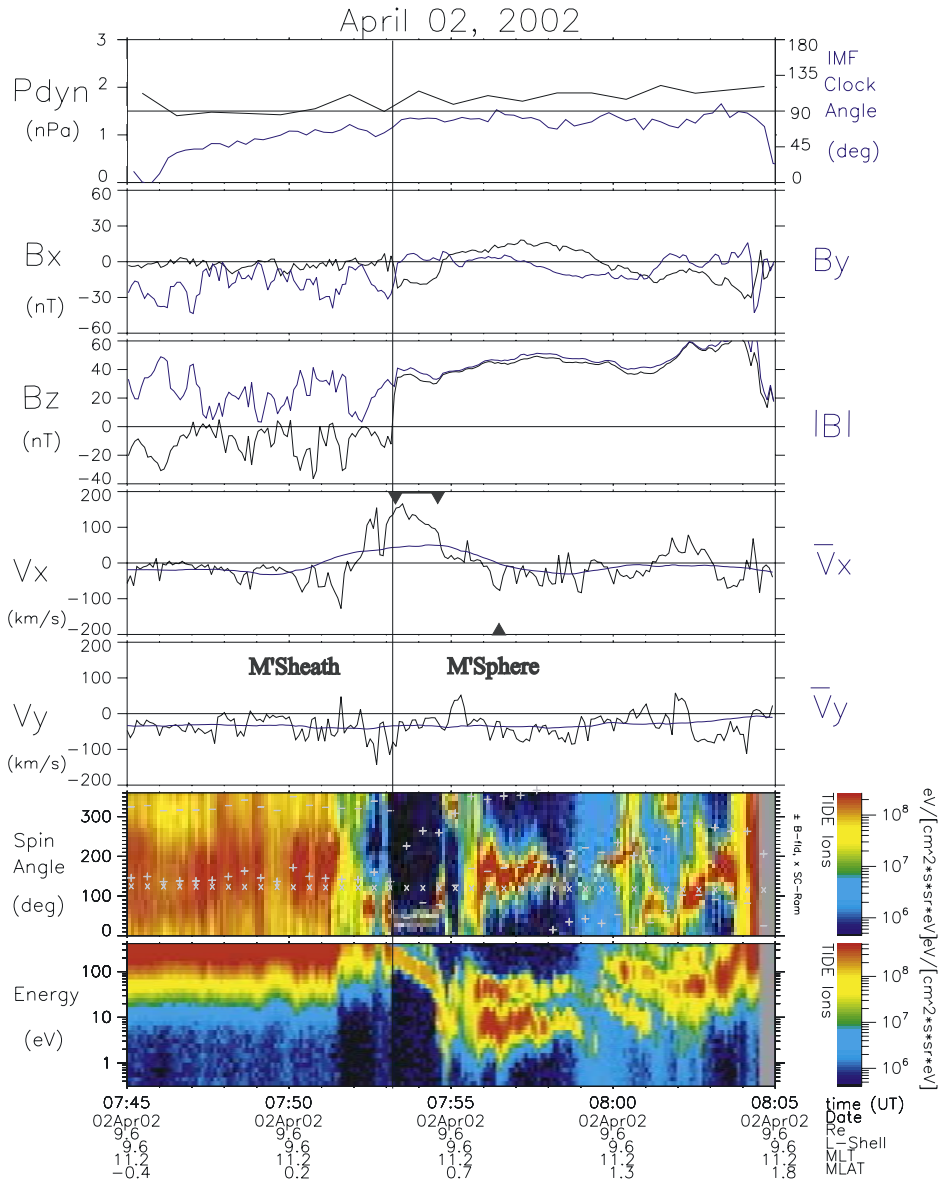

Figure 2. Time series stack plot for the event on 2 April 2002. From top to bottom, ACE/SWE solar wind dynamic pressure (black curve), ACE/MFI IMF clock angle (blue curve) in GSM (+90°, duskward or $B_y > 0$; −90°, dawnward or $B_y < 0$), Polar/MFE magnetic field components B_x (black curve), B_y (blue curve), and B_z (black curve) in GSM and field strength (blue curve), Polar/TIDE velocity components V_x and V_y (black curves) and their 5 min running averages (blue curves), Polar/TIDE ion spectrogram in spin-angle versus time and energy versus time. The magnetic field direction (plus sign), opposite direction (minus sign) and spacecraft motion direction (cross sign) in the upper panel are overlaid. The color bar indicates the differential flux in ions $cm^{-2}\ s^{-1}\ sr^{-1}\ eV^{-1}$ in logarithmic scale. Solar wind data is shifted in time to adjust the time lag between ACE and Polar. The black arrows mark the times the ion distributions are analyzed for ion species separation.

surveyed all the Polar apogee passes in the years of 2001 and 2002 when the spacecraft was at the dayside and near the equatorial plane. Important signatures to which we paid attention in selecting these events included: long periods of clearly identified magnetosheath intervals at the beginning or the end of the event (to ensure that the spacecraft was unambiguously near the magnetopause), multiple magnetopause crossings (to ensure the spacecraft stayed near the magnetopause for a relatively long period of time), and variability of ion fluxes inside the magnetopause. A total of 18 Polar magnetopause crossings were selected as meeting these criteria. Among these, only six events were studied in detail but all the 18 events were used to do a statistical study of the response of the magnetopause motion to the slow or long-term variations in the solar wind dynamic pressure. The statistical study was used as a base of reference to the more rapid or short-term variations of the magnetopause motion in response to the IMF and/or other upstream solar

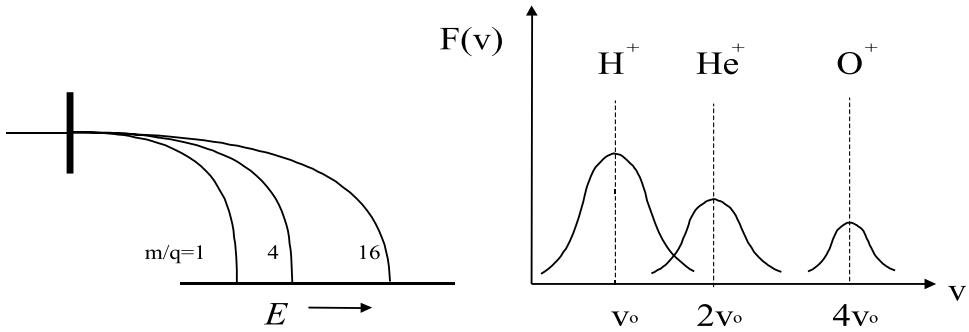

Figure 3. Schematic of the separation in E/q of three species having a common bulk velocity perpendicular to the background magnetic field relative to the spacecraft. Varying thermal speeds are analyzed by fitting the multiple E/q peaks with Maxwellian velocity distributions. H^+, He^+, and O^+ have E/q ratio of 1, 4, and 16, respectively. If observed, when plotted as an H^+ velocity distribution, there will be peaks at twice (He^+) or four times (O^+) the velocity of H^+.

wind drivers. Table 1 lists the times and locations in the magnetosphere as well as geomagnetic indices *AE*, *Dst*, and *Kp* for the six events. Measurements for three events representing three distinctive types of boundary oscillations are shown and discussed in detail below: 2 April 2002 (solitary), 20 March 2001 (irregular), and 7 February (quasi-periodic). The other three events are similar to the event on 20 March 2001 and classified as boundary oscillations with

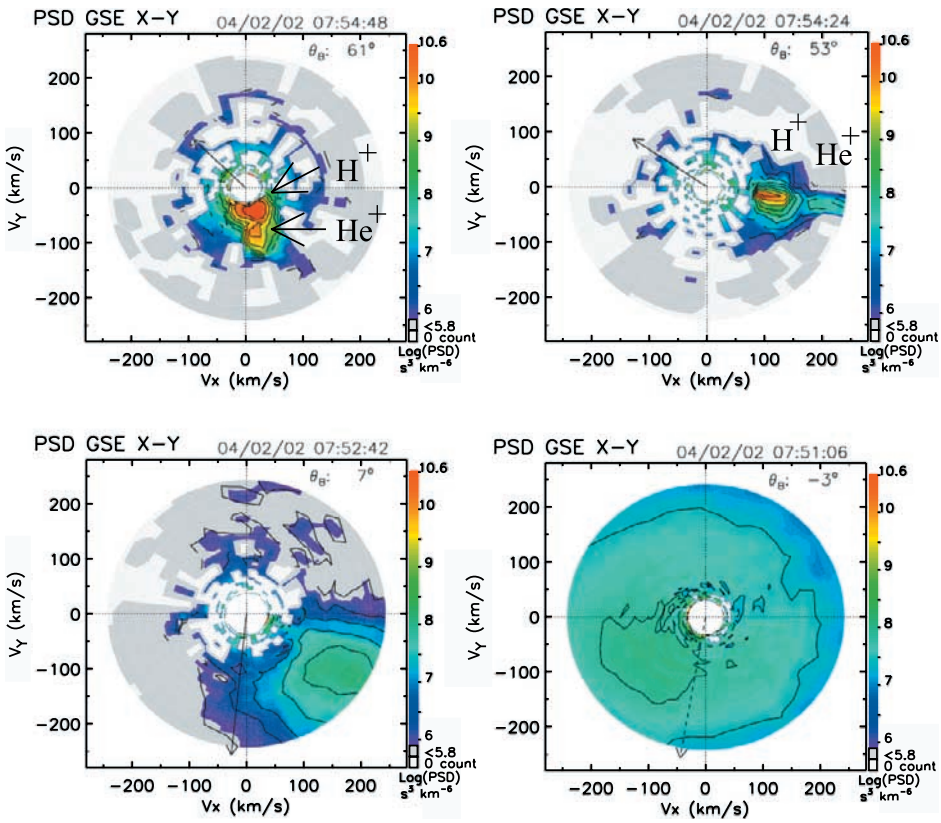

Figure 4. 6-s snapshot of ion velocity distributions in X-Y GSE plane for four selected intervals in the event on 2 April 2002. The spin plane is oriented within 3° from the X-Y GSE at the time. Projections of magnetic field unit vectors are shown in solid (above the spin plane) or dashed arrows (below the spin plane). The angles of the magnetic fields to the spin planes (θ_B) are printed at the upper right corners. The color tones are power spectrum density (PSD, s^3 km^{-6}) in logarithmic scale as shown to the right in each panel. In addition to colors, two levels of gray scales are applied to PSD of less than 5.8 (darker) in logarithmic scale and zero count or those below instrument noise level (lighter), respectively. Contours are overlaid at each 0.5 level. From left to right, upper then lower panels, it shows velocity distributions for the intervals of magnetosphere (0754:48 UT), LLBL-magnetosphere proper (0754:24 UT), LLBL-Magnetosheath proper (0752:42 UT), and magnetosheath (0751:06 UT).

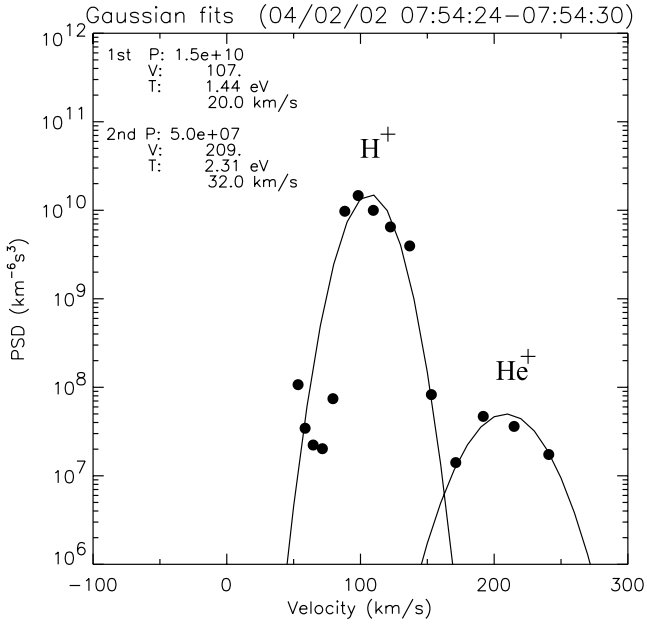

Figure 5. Result of ion species separation analysis for the event on 2 April 2002. Using Levenberg-Marquardt method, two Gaussian curves are used to fit the one-dimensional (1-D) distribution function taken from the slice of 2-D ion distribution function containing the peaks of power spectrum density.

irregular time period. All six events are summarized below in formats pertinent to particular physical processes.

[7] Figure 1 shows the positions of magnetopause crossings by Polar in our data set. The upper panel shows them in magnetic latitude versus magnetic local time. The lower panel shows these positions projected onto the magnetic equator. The circled dots represent the events for which flow bursts were observed as listed in Table 1. The position of a model magnetopause [*Shue et al.*, 1997] at solar wind dynamic pressure of 3 nPa and IMF $B_z = -5.0$ nT is shown for reference. The orbital coverage for the events studied ranged from 6 to 18 hours in magnetic local time and within ±45° in magnetic latitude. The average position of the magnetopause was near the Polar apogee of ~9 R_E, which is consistent with the medium level of geomagnetic activity with $Kp \sim 4$ with the magnetopause moderately compressed and/or eroded. In addition to the selection criteria described in the introduction, the events were limited to the seasons when Polar apogee passes were near the magnetopause and consequently not far away from the Sun-Earth line, as the magnetopause flares out at high latitudes and earlier or later local times. The orbital sampling distribution for this set of events was not uniform enough to reach firm conclusions about the distribution of such flow events on the magnetopause.

[8] Figure 2 shows a time series stack plot for the event on 2 April 2002. The time lag is calculated based on the convection time between the ACE at L1 and the center of Earth, the distance divided by the Sun-Earth component of solar wind speed. The high flux level near the high-energy cutoff at the beginning of the interval indicates magnetosheath plasma. The fluxes then shifted to lower energies and were much more confined in energy after the spacecraft went into the magnetosphere. Intervals of solitary flow bursts were seen near 0753–0755 UT and toward the end of the interval at 0803–0805 UT when the B_x component of the magnetic field became negative and therefore when the field orientation deviates from the typical northward magnetospheric magnetic field, where B_x and B_y are small near the equatorial plane. The IMF clock angle was near 90° and remained relatively steady through out the interval. The solar wind pressure displayed a slowly increasing trend. The magnetopause was expected to be relatively steady. This indicates that the sunward flow bursts were caused by physical processes other than an expansion of the magnetosphere, which could be produced by an abrupt decrease but not by an increase in solar wind pressure. Since the IMF B_x component is comparable with the other two components (IMF was ~43° from the Sun-Earth line), the possible abrupt decrease in the solar wind pressure in the foreshock, however, was not totally ruled out as a contributor to the sunward flow.

[9] We employ the common velocity assumption to identify ion species in velocity distributions. Figure 3 shows a schematic of the separation in E/q of three species having a common bulk velocity perpendicular to the background magnetic field relative to the spacecraft. Varying thermal speeds are analyzed by fitting the multiple E/q peaks with Maxwellian velocity distributions. H^+, He^+, and O^+ have E/q ratio of 1, 4, and 16, respectively. This assumption is justified when, plotted as an H^+ velocity distribution, there are peaks at twice (He^+) or four times (O^+) the velocity of H^+. Figure 4 shows 6-s snapshots of ion velocity distributions in X-Y GSE plane for four selected intervals in the event shown in Figure 2. We keep the definition of boundary layer loose as the plasma properties differ in detail from one pass to another. We simply put the magnetopause at the point where the magnetic field configuration changes from magnetospheric to magnetosheath-like, with the magnetosphere (magnetosheath) proper earthward (sunward) from the magnetopause. We used the Levenberg-Marquardt method with constrains on the combination of the coefficients, peaks, widths, and displacements. We used one, two, or three Gaussian curves to fit 1-D distribution functions taken from slices of 2-D distribution functions containing peaks of power spectrum density. Figure 5 shows a sample result of the analysis. The true velocity of the plasma is characterized by the displacement of the Gaussian curve fitting the maximum peak, as determined by the moment calculation, for the selected intervals as shown in the velocity panels of Figure 3. In the magnetosphere proper, two species are identified: H^+ and He^+. In the magnetosphere, ions flow mainly dawnward at 50 km s^{-1}. While in the boundary proper, the two species are accelerated toward the magnetopause at speed >100 km s^{-1} and near 150 km s^{-1} at the magnetopause. The speed relative to the magnetopause could be slightly higher as the magnetopause is pushed in due to the slow increase in the solar wind pressure at <5 km s^{-1}. In the magnetosheath proper, we have a heated plasma, possibly magnetospheric H^+, on magnetosheath-like field flowing around the magnetopause before encountering magnetosheath plasma with much higher fluxes and exceeding the energy range of the instrument. The duskward flow in the magnetosheath, as well as in the magnetosphere at much slower speeds, is

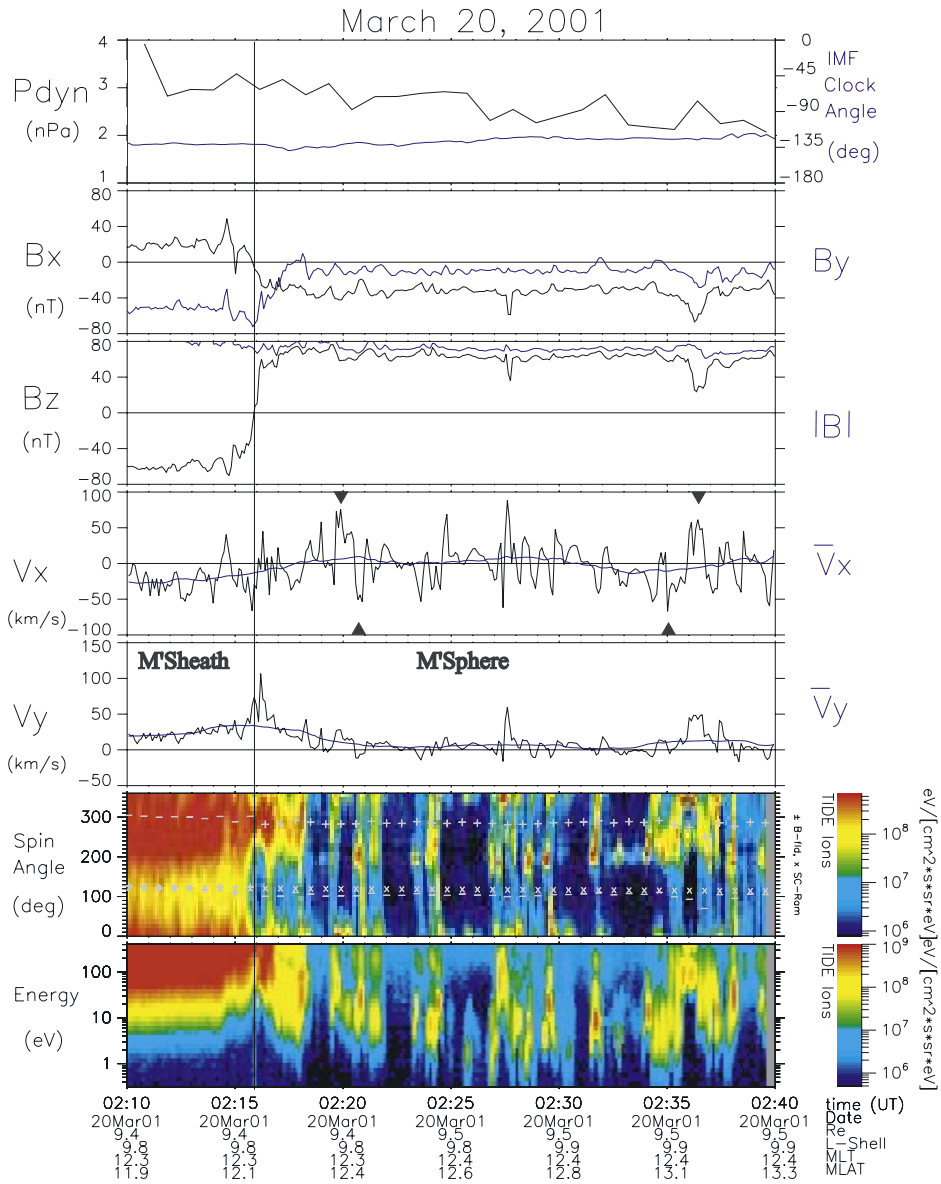

Figure 6. Time series stack plot for the event on 20 March 2001. The panel layout is the same as Figure 2. Time lag between Polar and ACE is adjusted accordingly to make the plot.

consistent with the location of Polar being near the equatorial plane and not far away from the Sun-Earth line.

[10] The distinctive single rapid sunward motion of the magnetospheric magnetic fields we have just seen is not common in our study, either not commonly present or not easily observed. With four out of six events analyzed in detail, the motion of the magnetospheric magnetic fields characterized by the velocity of the cold plasma is somewhat periodic but highly irregular. Figure 6 shows the time series stack plot for the event on 20 March 2001 that exemplifies this nature. The panel layout is the same as Figure 2. The time lag between Polar and ACE is adjusted accordingly to make the plot. The IMF clock angle was near $-135°$ and relatively steady through out the interval. The solar wind pressure is in a decreasing trend accompanied by small fluctuations. The intervals of 80 km s^{-1} or greater flow speed bursts occur near 0219 and 0236 UT when the magnetic field orientations deviate from the typical magnetospheric northward magnetic field. The sunward expansion of the magnetosphere due to the slow decrease in solar wind pressure is around 20 km s^{-1} or less as observed in the magnetosphere (the 5-min running averages, blue curve, in the V_x panel of Figure 6). The earthward motions of the magnetic fields in the opposite cycles reveal intermediate velocities at $\sim$50 km s^{-1}. In contrast, the velocities of the sunward flow bursts are distinctively higher. Combining the evidence of changes in the magnetic field orientation and flow acceleration, we suggest that this is a phenomenon that is not accounted for in terms of slow expansion of the magnetosphere. The effect of pressure variation in the foreshock was not likely to be important, as the IMF B_x was a small component, with the IMF $\sim$82° from the Sun-Earth line.

[11] Figure 7 shows the ion velocity distributions for the event on 20 March 2001. The spin plane of the spacecraft is about 31° from the X-Z GSE plane. The format of the figure

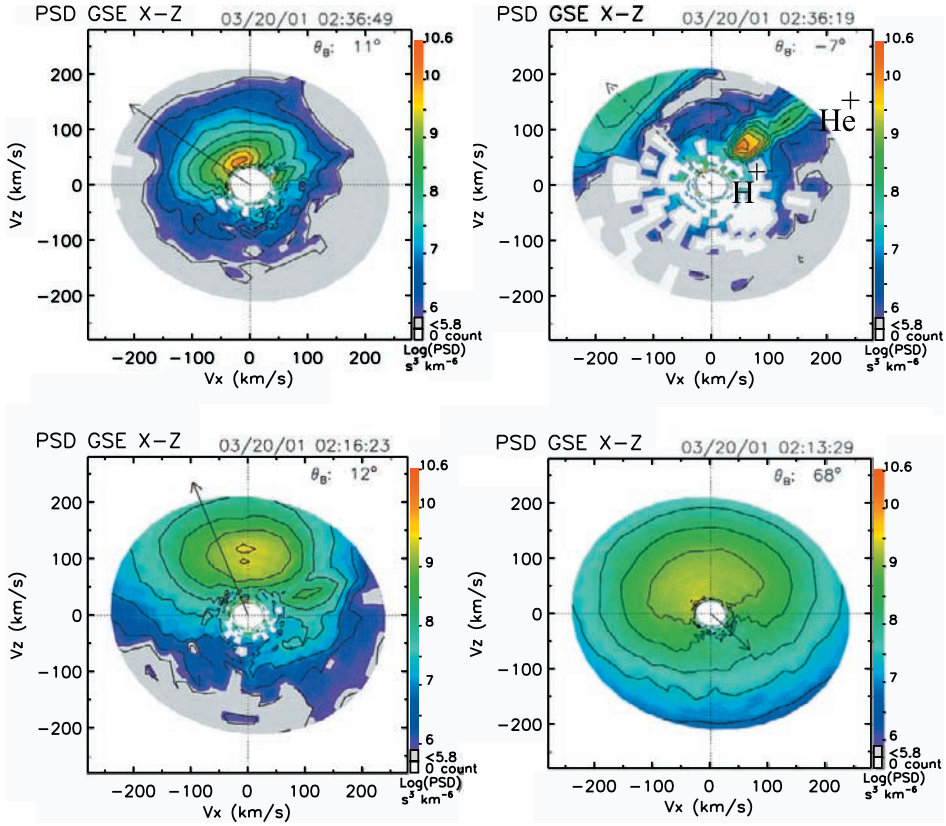

Figure 7. 6-s snapshot of ion velocity distributions for the event on 20 March 2001. The format of the figure is the same as Figure 4 except plotted in X-Z instead of X-Y plane. The spin plane of the spacecraft is about 31° from the X-Z GSE plane at the time. From left to right, upper then lower panels, it shows ion velocity distributions for the intervals of magnetosphere (0236:39 UT), LLBL-magnetospheric proper I (0236:19 UT), LLBL-magnetospheric proper II (0216:23 UT), and magnetosheath (0213:29 UT).

is the same as Figure 4 except that it is plotted in X-Z instead of X-Y plane. It shows a 6-s snapshot of the ion velocity distribution for plasmas in the magnetosphere (0236:39 UT), LLBL-magnetospheric proper I (0236:19 UT), LLBL-magnetospheric proper II (0216:23 UT), and magnetosheath (0213:29 UT). In the magnetosphere the velocity distribution is stretched in the azimuthal direction because of the collapsing of 3-D distributions into the spin plane (see instrument introduction in this paper). However, it is barely distinguishable from a temperature isotropy that stretches either perpendicular or parallel to the magnetic field, indicating the existence of a velocity component perpendicular to the spin or X-Z plane. The direction of the flow is either dawnward or duskward at a speed less than 50 km s^{-1}. In the LLBL-magnetospheric proper I (0236 UT), H^+ and He^+ are identified as dominant components (Figure 7 and 8). In addition to cold H^+ and He^+ there is another plasma component flowing somewhat northward and extending beyond the energy range of the instrument. In the LLBL-magnetospheric proper II, a mixture of cold plasmaspheric and hot magnetosheath plasmas is seen. The hot plasma component is flowing northward with a finite velocity component perpendicular to the X-Z plane. However, the mixture of two populations in a 6-s snapshot is not conclusive as time aliasing is possible. In the magnetosheath, ion flux increases dramatically and the magnetic field was oriented close to the IMF direction. The plasma

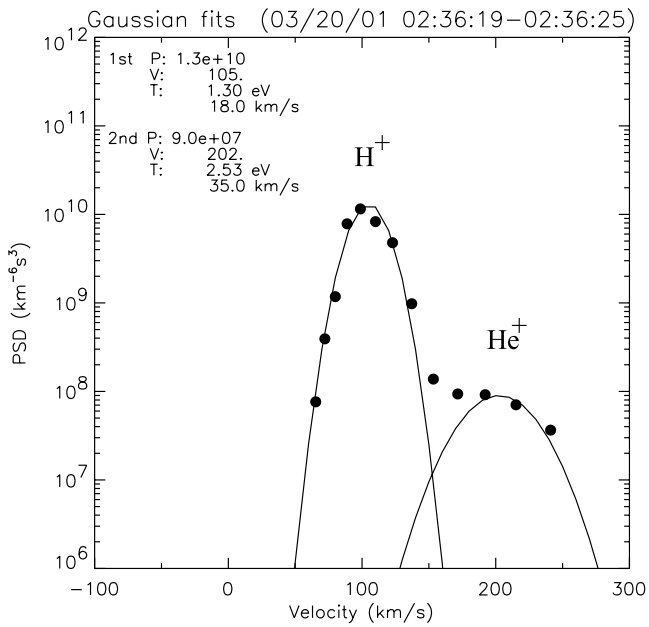

Figure 8. Result of ion species separation analysis for the event on 20 March 2001. The method of analysis and displaying format are the same as Figure 5.

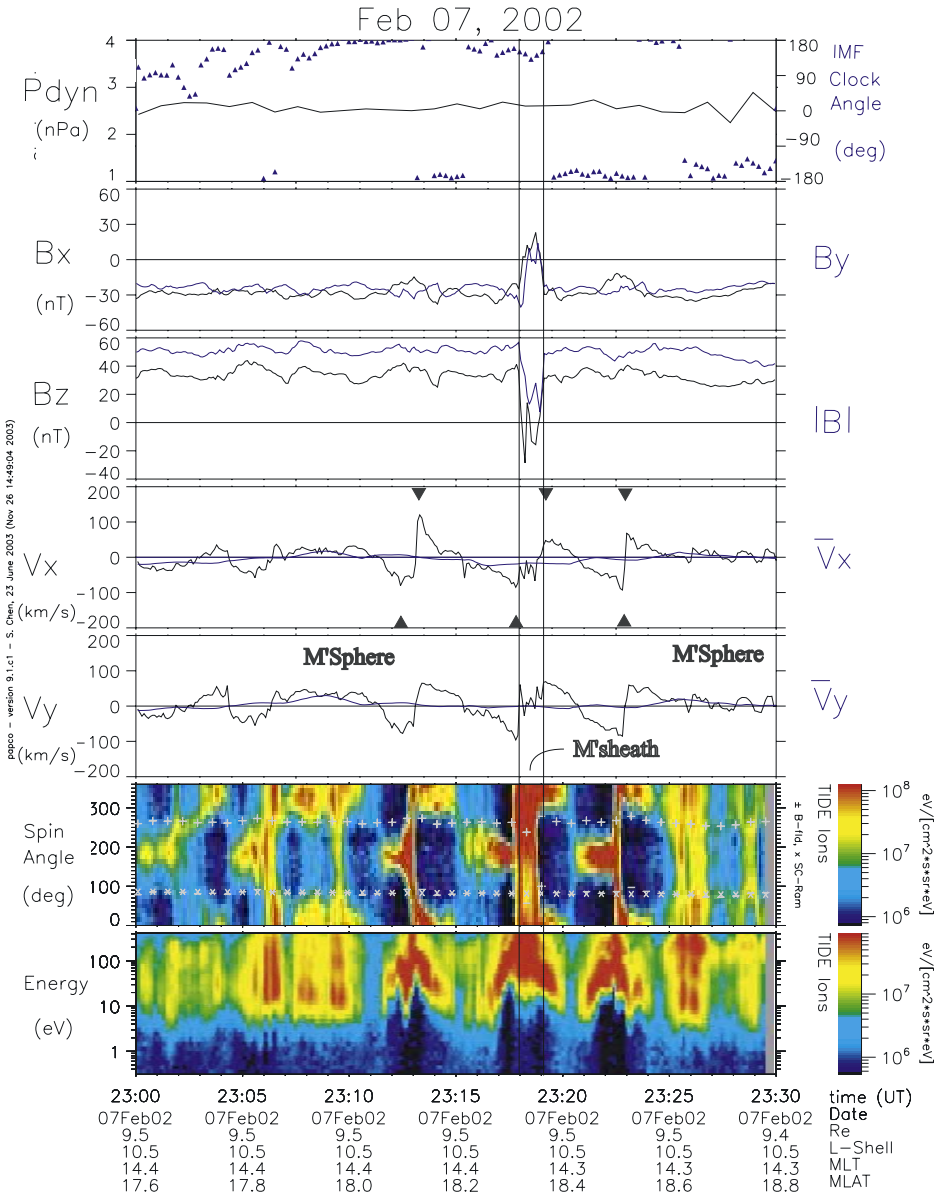

Figure 9. Time series stack plot for the event on 7 February 2001. The panel layout is the same as Figure 2 except using symbols instead of a continuous curve are used to represent the clock angle. Time lag between Polar and ACE is adjusted accordingly to make the plot.

flows northward with a component perpendicular to the X-Z plane indicated by the stretching of contours in the azimuthal direction. Since Polar was at 12.4 hours MLT and +13° MLAT, the flow direction is more northward and slightly duskward (instead of dawnward).

[12] Although in most cases the period of the motion of the magnetospheric magnetic field just inside the magnetopause varies, we found a case in which the period is near constant. Figure 9 shows time series stack plot for the event on 7 February 2002 when a quasi-periodic motion of the magnetospheric boundary was observed. Polar spacecraft encountered the magnetosheath plasma between 2317:50 UT and 2318:50 UT during an oscillation cycle before and after a series of periodic boundary motions just inside the magnetopause. The B_z component became negative in the magnetosheath, consistent with the strongly southward IMF (the clock angle was near ±180°). The IMF was ~25° from the Sun-Earth line, and therefore B_x was the dominant component during this interval. The pressure variation in the foreshock region is likely to be one of the important factors in establishing the quasi-periodic oscillation. Figure 10 shows 6-s snapshot of ion velocity distributions for the intervals: magnetosphere (2316:24 UT), LLBL-magnetosphere I (2317:42 UT), magnetosheath (2318:50 UT), and LLBL-magnetosphere I (2319:18 UT). The spin plane of the spacecraft was about 50° from the X-Z GSE plane at the time. The out-of-spin-plane component of flow velocity (azimuthal spreading in velocity distributions) could be important in

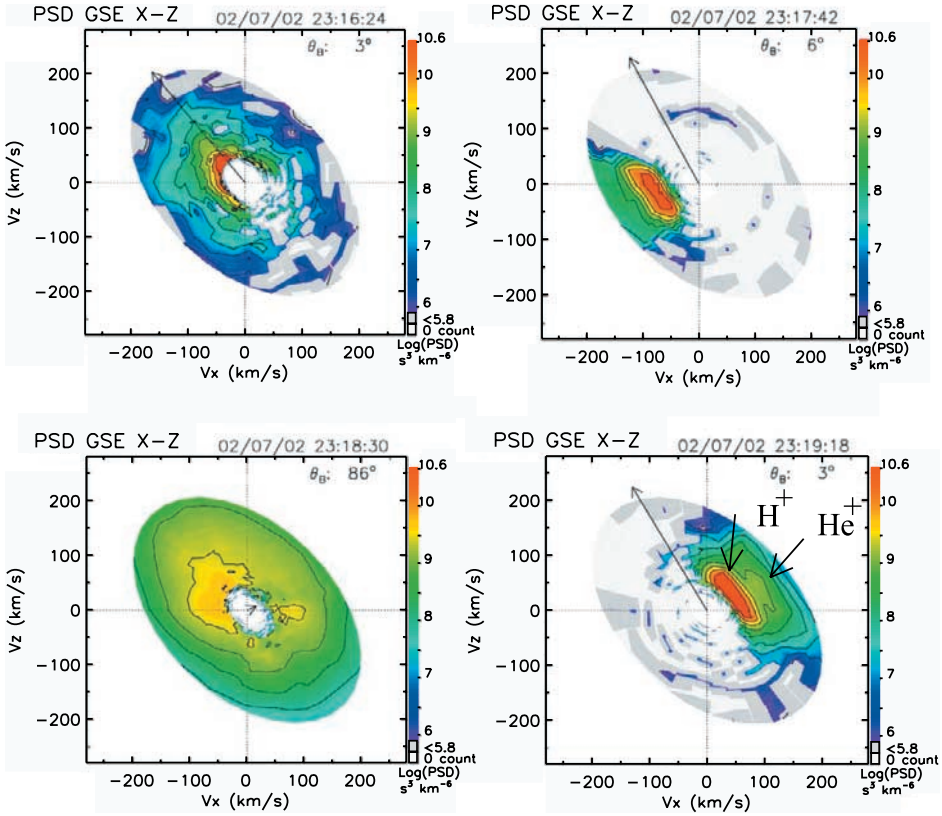

Figure 10. 6-s snapshot of ion velocity distributions for the event on 7 February 2002. The format of the figure is the same as Figure 4 except plotted in X-Z instead of X-Y plane. The spin plane of the spacecraft is about 50° from the X-Z GSE plane at the time. From left to right, upper then lower panels, it shows ion velocity distributions for the intervals of magnetosphere (2316:24 UT), LLBL-magnetosphere I (2317:42 UT), magnetosheath (2318:50 UT), and LLBL-magnetosphere I (2319:18 UT).

estimating the inward and outward motion of the magnetopause boundary layer at 14.3 hours local time (35° from the noon-midnight plane). In the magnetosphere (2316:24 UT) the flow was mostly field aligned. In the magnetosheath (2318:50 UT), the flow direction was near perpendicular to the magnetic field and about 20° from the Z-axis, which is consistent with the nominal magnetosheath flow at 18° in latitude. In the LLBL-magnetosphere I intervals (2317:42 UT and 2319:18 UT), the flows were mostly perpendicular to the magnetic field. The outward and inward motions were near symmetric in terms of velocity and waveform. Two ion species, H^+ and He^+, were identified in some of these intervals (Figure 11). The ion distribution functions at the times when the velocity peaks occur for three wave cycles (near 2313 UT, 2328 UT, and 2334 UT) are analyzed and discussed in detail below.

[13] Two out of six events were found to contain three ion species, H, He^+, and O^+. Figure 12 shows the ion species separation analysis for the event on 5 March 2002. The apparent velocities for the three ion species are 38, 75, and 140, respectively, corresponding to the ratios of 1.0, 1.97, and 3.6. The result is in good agreement with the E/q ratios of 1, 4, and 16 for H^+, He^+, and O^+, respectively. Another event that contained the three ion species was on 14 May 2002, but the ratios of the velocity displacements were not as clear. Table 2 lists the coefficients of the fits to Gaussian

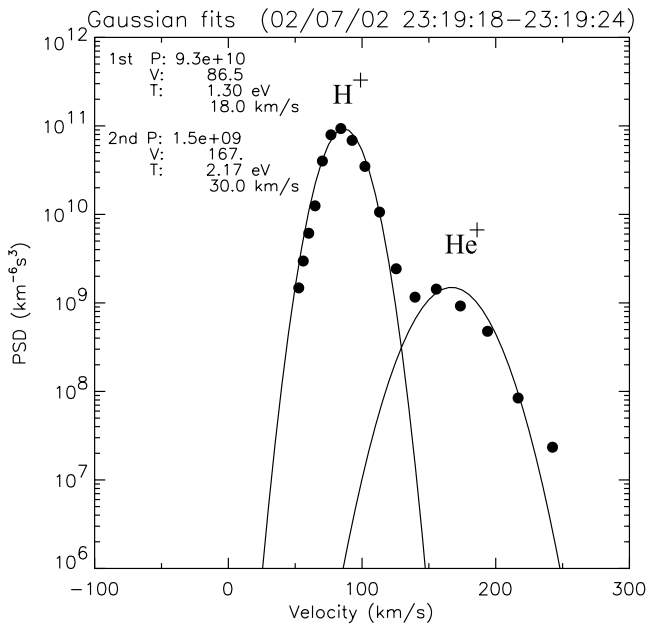

Figure 11. Result of ion species separation analysis for the event on 7 February 2002. The method of analysis and displaying format are the same as Figure 5.

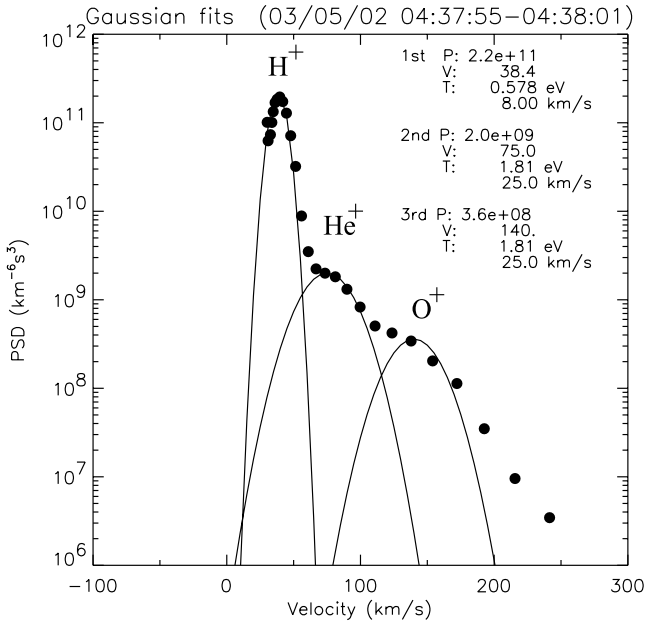

Figure 12. Result of ion species separation analysis for the event on 5 March 2002. The method of analysis and displaying format are the same as Figure 5 except analyzed and shown a possible third component O^+.

curves at selected cycles of inbound and outbound motions of the magnetic field or magnetospheric boundary for all the six events. The sign of the number under the In/Out column in each fitting indicates the direction of the velocity, positive for outbound and negative for inbound, while the value indicates how many species were present. In place of values of the coefficients for the second and the third sets, ratios with respect to the first set are shown. If the second or the third peak of a distribution was near or below the sensitivity of the instrument, a question mark is given. This occurs when the consecutive distributions before or after indicate the presence of additional ion species. Attached for each distribution are the spin integral plasma density moment, spin-averaged magnetic field strength, derived Alfvén speed, and Alfvén Mach number. For five out of six events the ratios of the velocities between He^+ and H^+, V_1/V_0, are ~2.0, consistent with the prediction of common ion species velocity. The concentration of He^+ relative to H^+ is mostly a few percent, except the last two entries in 14 May 200. The apparent velocity ratios, V_1/V_0, are a bit off the common velocity expectation for He^+ to H^+. In summary, for all the six events the number densities of these cold ion species range from 1 to 100 cm^{-3}. The Alfvén speeds range from 100 to 1000 km s^{-1}. The Alfvén Mach numbers are mostly above 0.1 and as high as 0.6. Table 3 summarizes these plasma parameters, the derived convection electric field, $V_x \times B_z$, the solar wind dynamic pressure, and *Kp* index during these events.

[14] Solar wind dynamic pressure is the major driver of the motion of the subsolar magnetopause. Its variation in any timescale could launch a spectrum of waves in the magnetosphere. Even if it is relatively steady upstream, when the IMF B_x is the dominant component it could be disturbed downstream of the Earth's bow shock and still launch another set of variations that drive the magnetopause to oscillate. To better understand the degree to which the sunward flow bursts can be understood merely as a simple wave motion due to these two causes, we first remove the effect due to the variation of solar wind dynamic pressure upstream. We then study the boundary motion as a function of IMF orientation. We correlate the variation of solar wind pressure with the motion of the subsolar magnetospheric boundary layer, characterized by the motion of cold plasma just inside the magnetopause. The intervals of cold plasma just inside the magnetopause are selected based on the statistics of temperature and density in the database consisting of the 18 events. A simple equation with two parameters is applied to separate the group of magnetospheric ions from the one for magnetosheath ions. Relationships are calculated for the cumulative variations in solar wind dynamic pressure ΔP_{dyn} over the time intervals of 10 min, 20 min, and 30 min, centered at the correct time lags, versus the flow speeds of the magnetospheric ions. We then calculated the correlation coefficients of linear least squares fit for each of the cases with various IMF clock angles and integration durations (Table 4). Only the case with the 30 min duration shows a correlation (-3.6 km s^{-1} nPa^{-1} ΔT^{-1}) that is above its standard deviation during northward IMF ($\Theta < 45$). Figure 13 shows a plot of the relationship. Three panels represent three categories of IMF clock angles: northward IMF ($|\Theta| < 45°$), horizontal IMF ($45° \leq |\Theta| \leq 135°$), and southward IMF ($135° < |\Theta|$). The result of linear least squares fit for the corresponding categories is shown in each panel. Assuming the solar wind dynamic pressure decreases by 1 nPa over 30 min and the IMF is northward, the magnetopause expands at a speed of 3.6 km s^{-1} and the magnetopause will move out 1 R_E over the period. We find a weak or negligible correlation for the cases with horizontal or southward IMF and all those with shorter integration times. With highly scattered distributions, this indicates other important factors, such as the orientation of IMF in driving the motion of the magnetopause on timescale of 30 min or less. All the six events studied for the sunward flow bursts show slow varying solar wind dynamic pressure at less than 2 nPa over the 30 min period or longer, corresponding to less than 10 km s^{-1} inward or outward speed. *Mozer et al.* [2002] estimated the magnetopause motion at a speed of ~24 km s^{-1} based on an averaged $\mathbf{E} \times \mathbf{B}$ convection speed (both $\mathbf{E}$ and $\mathbf{B}$ were measured) over a single pass (not over a full wave cycle) across the magnetopause. The event shown in their paper however is an extreme case in the presence of pressure pulse, the solar wind dynamic pressure increased by ~2 nPa and dropped to a value slightly below the starting level within 20 min. Their study could provide an upper bound of the magnetopause motion speed due to a more rapid change in the solar wind dynamic pressure.

[15] Figure 14 shows velocity deviations as a function of IMF clock angle (upper panel) and cone angle (lower panel) for the six events studied. The cone angle is defined as the angle between IMF and Sun-Earth line and is less (greater) than 90° when the IMF is pointing toward (away) from the Sun. The velocity deviation ΔV is obtained by subtracting the velocity for outward/sunward moving flux tube from those for inward/earthward in a wave cycle. Positive (negative) ΔV represents outward/sunward (inward/earthward)

Table 2. List of the Coefficients of Fits to Maxwellian Distribution and Plasma Parameters for the Time Intervals Studied

Time, UT		In (−)/ Out (+)	F_0, s^3 km^{-6}	V_0, km s^{-1}	T_0, eV	F_1/F_0, %	V_1/V_0	F_2/F_0, %	V_2/V_0	n_1/n_0, %	N, cm^{-3}	$\|B_{sp}\|$, nT	V_A, km s^{-1}	M_A
20 March 2001	02:19:53	2	2.1E+10	88.2	1.9	0.4	2.0	–	–	0.9	52.0	73.0	223	0.40
	02:20:41	−1	2.5E+11	48.8	1.1	–	–	–	–	0.0	14.9	67.0	383	0.13
	02:35:07	−1	3.6E+12	23.6	1.1	–	–	–	–	0.0	42.6	69.3	234	0.10
	02:36:07	2	2.6E+10	104.4	1.9	0.3	1.8	–	–	0.7	7.8	75.2	592	0.18
	02:36:13	2	5.9E+09	131.3	1.6	1.0	1.6	–	–	1.9	4.1	75.3	818	0.16
	02:36:19	2	1.3E+10	105.0	1.3	0.7	1.9	–	–	1.7	4.6	72.6	742	0.14
7 February 2002	23:12:30	−2	3.1E+10	111.9	1.9	0.8	1.9	–	–	0.9	21.6	52.8	250	0.45
	23:13:18	1	2.7E+10	148.3	1.2	–	–	–	–	0.0	20.8	49.6	239	0.62
	23:17:42	−2	5.4E+10	110.2	1.4	0.5	2.0	–	–	0.8	43.8	54.2	180	0.61
	23:19:18	2	9.3E+10	86.5	1.3	1.6	1.9	–	–	2.7	47.1	49.5	159	0.55
	23:22:06	−2	8.1E+10	93.5	1.3	0.7	1.9	–	–	1.4	44.5	46.9	155	0.60
	23:23:12	2	1.2E+11	80.6	1.1	1.2	2.0	–	–	1.5	44.1	49.0	162	0.50
17 February 2002	04:45:09	2	1.7E+10	91.4	2.5	3.4	2.0	–	–	4.9	19.0	87.9	444	0.21
	04:48:09	−2	1.0E+12	39.4	0.9	0.7	2.0	–	–	1.4	51.0	83.1	256	0.15
	05:23:28	2	3.9E+10	72.7	1.3	12.5	1.5	–	–	12.5	23.9	83.7	377	0.19
	05:24:10	−3	3.6E+11	29.6	0.7	4.3	2.2	0.52	3.4	6.9	19.1	83.5	420	0.07
5 March 2002	04:12:06	2	1.8E+11	46.5	0.7	1.4	1.9	–	–	4.3	23.5	74.6	339	0.14
	04:25:36	−3	7.1E+11	45.5	0.6	0.4	2.0	0.03	3.7	1.1	39.0	68.2	240	0.19
	04:37:55	3	2.2E+11	38.4	0.6	0.9	2.0	0.16	3.6	2.8	10.4	62.4	427	0.09
	04:39:07	−3	7.1E+11	46.5	0.6	0.7	1.9	0.04	3.7	2.1	27.4	84.6	356	0.13
2 April 2002	07:53:18	1	1.2E+09	181.0	1.8	?	?	–	–	?	2.9	40.9	531	0.34
	07:53:24	1	2.5E+09	171.0	1.8	?	?	–	–	?	2.6	40.1	545	0.31
	07:53:30	1	2.5E+09	182.0	1.6	?	?	–	–	?	2.6	39.2	531	0.34
	07:53:36	1	1.5E+09	159.0	1.6	?	?	–	–	?	3.3	39.9	486	0.33
	07:53:42	1	3.0E+09	145.0	1.6	?	?	–	–	?	3.5	41.2	485	0.30
	07:53:48	2	5.0E+09	142.0	1.3	1.0	1.9	–	–	2.0	3.1	40.4	506	0.28
	07:53:54	1	5.0E+09	143.0	1.8	?	?	–	–	?	3.5	38.9	459	0.31
	07:54:00	1	4.0E+09	143.0	1.6	?	?	–	–	?	4.3	37.7	401	0.36
	07:54:06	2	4.8E+09	128.0	1.3	0.8	1.9	–	–	1.7	3.2	36.9	455	0.28
	07:54:12	2	1.1E+10	121.0	1.4	0.1	1.8	–	–	0.1	4.8	36.7	368	0.33
	07:54:18	2	1.8E+10	112.0	1.1	0.7	1.9	–	–	1.8	4.9	35.4	354	0.32
	07:54:24	2	1.5E+10	107.0	1.4	0.3	2.0	–	–	0.5	5.1	33.4	326	0.33
	07:56:24	−2	1.0E+12	38.4	0.7	5.1	2.0	–	–	7.7	102.4	46.5	101	0.38
14 May 2002	06:24:37	−2	1.2E+10	57.2	0.7	3.3	1.6	–	–	4.9	2.2	55.8	822	0.07
	06:25:01	1	7.8E+08	146.4	2.2	–	–	–	–	0.0	1.8	50.2	821	0.18
	06:47:44	3	4.0E+08	70.7	0.9	24.9	1.5	1.73	2.5	51.9	1.9	47.4	763	0.09
	06:48:32	−3	4.5E+08	75.8	1.0	19.0	1.6	1.62	2.8	34.0	1.4	51.9	983	0.08

motion. Most outward flow bursts occurred when the clock angles were near ±180°, i.e., southward IMF, except those observed in 2 April 2002 (open circles) when the IMF orientation was mostly horizontal. The IMF cone angle, however, did not exhibit a trend, suggesting that pressure variations from the foreshock are not a cause of outward flow bursts. This would be important when the cone angle is near 0° or 180°. While the 2 April 2002 event requires further study, most of our cases are better explained as the magnetic reconnection being the major cause of the outward/sunward flow bursts.

3. Discussion

[16] We report sunward flow bursts just inside the subsolar magnetopause at speeds of up to ∼100 km s^{-1} in excess of the averaged speed of the boundary oscillations. We estimated their densities at 1–100 cm^{-3} and particle fluxes at 0.1–4.8 × 10^8 ions cm^{-2} s^{-1}. The ions are composed of H^+ (>90%), He^+ (<10%), and possibly a trace of O^+. This is comparable with earlier observations of H^+ (99%), He^+ (1%), and O^+ (0.1%) in the outer magnetosphere using OGO-5 data [*Chappell et al.*, 1970] and observations of He^+ dominant over O^+ in the subsolar magnetopause boundary layer using ISEE Energetic Ion Mass Spectrometers [*Peterson et al.*, 1982]. The convection electric field of ∼4 mV m^{-1} is much larger than the average of 0.4 mV m^{-1} of the same level of geomagnetic activities but extends over a much wider range in local times in the outer magnetosphere [*Rowland and Wygant*, 1998]. Assuming the total cross section of the

Table 3. Summary of the Ranges of Plasma Parameters of the Flow Bursts Studied

Parameter	Value Range (Median)
N, cm^{-3}	1.4–102 (7.8)
$T_{core\ H^+}$[a], eV	0.6–2.5 (1.3)
V, km s^{-1}	23–182 (104)
N_{He^+}/N_{H^+}[b], %	0–12.5 (1.1)
NV, cm^{-2} s^{-1} × 10^8	0.1–4.8 (0.58)
M_A	0.07–0.62 (0.28)
$\|B_{sphere}\|$, nT	33–88 (50)
E, mV m^{-1}	1.4–7.2 (3.8)
$Pdyn_{sw}$, nPa	1.4–7.6 (2.2)
Kp	2^+–5^+ (4)

[a]Fitted to a single Maxwellian distribution function for H^+ within the optimal energy range of TIDE instrument.
[b]Excluding the last two entries in Table 2.

Table 4. List of Correlation Coefficients of Linear Least Squares Fits of Flow Speed Versus Cumulative Variation of Solar Wind Dynamic Pressure, $V_x = c0 + c1\ \Delta P_{dyn}$

ΔT, min	Θ_{IMF}, deg	c0, km $s^{-1}\Delta T^{-1}$	σ_{c0}	c1, km s^{-1} $nPa^{-1}\Delta T^{-1}$	σ_{c1}	Number of Points
10	<45	−2.4	±1.1	−0.8	±1.2	355
	45−135	2.0	±0.5	1.1	±0.4	1685
	135<	4.1	±0.8	0.3	±0.5	621
20	<45	−1.0	±1.7	−0.2	±1.2	214
	45−135	1.0	±0.6	−1.6	±0.5	1126
	135<	4.1	±0.9	−0.2	±0.5	528
30	<45	−5.9	±2.4	−3.6	±1.0	104
	45−135	1.2	±0.7	−0.8	±0.4	849
	135<	4.2	±1.0	−0.9	±1.2	389

sunward flow bursts carried by a flux tube is 10 R_E^2 with a size of ∼1 R_E in width and ∼10 R_E in length, measured between northern and southern cusp bifurcation points, the median number of particles brought to the dayside magnetopause is $\sim 2(0.4 - 20) \times 10^{26}$ ions s^{-1}, which is an appreciable fraction of incoming solar wind flux taken the same incident area with the averaged solar wind parameters of V_{sw} ∼400 km s^{-1} and n_{sw} ∼5 cm^{-3} or 2 nPa.

[17] Using Cluster Ion Spectrometry (CIS) on two of the Cluster spacecraft, *Sauvaud et al.* [2001] showed an event of cold dense (∼3 eV and 3–10 cm^{-3}) ions with the composition of H^+, He^+, and O^+ just inside the magnetopause at ∼8.6 hours local time and ∼42° latitude during weak geomagnetic activities (*AE* ∼50 nT). They showed that the ions were accelerated to a speed up to 140 km s^{-1} perpendicular to the magnetic field and produced a convection electric field of 2.8 mV m^{-1}. They interpreted it as an intermittent acceleration due to the motion of the magnetopause caused by the variation of solar wind dynamic pressure (∼25%) but did not exclude the possibility of

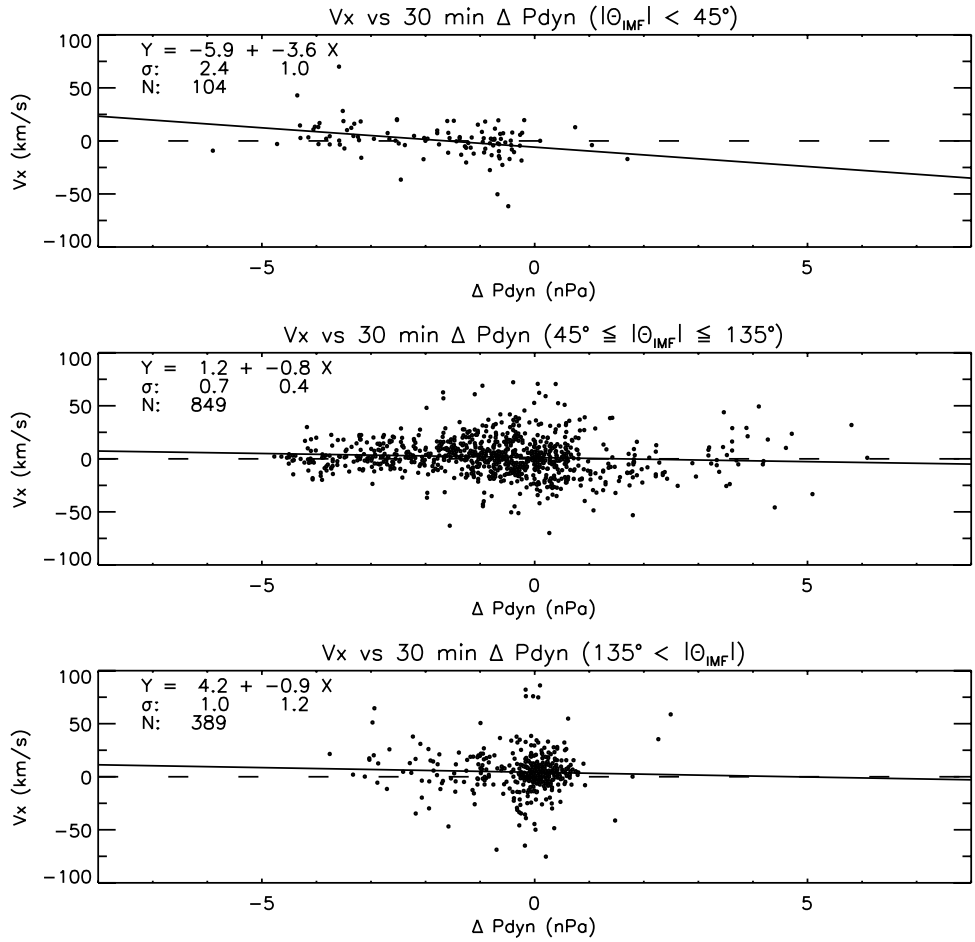

Figure 13. Relationship between the 30 min accumulative variations of solar wind dynamic pressure and the motion of the magnetopause characterized by the motion of the magnetic flux tubes just in side the magnetopause. Three panels represent three categories of IMF clock angles: northward IMF ($|\Theta| < 45°$), horizontal IMF ($45° \leq |\Theta| \leq 135°$), and southward IMF ($135° < |\Theta|$). Results of linear least squares fits for each of the categories are shown in each panel.

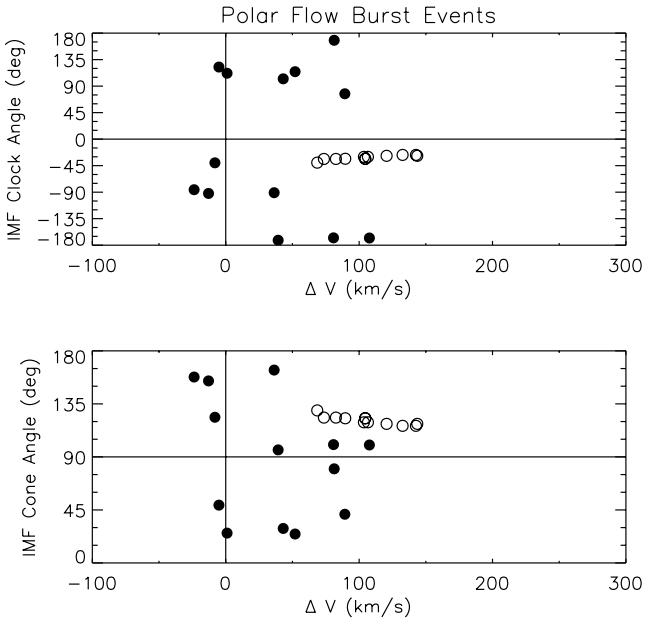

Figure 14. Velocity deviations as a function of IMF clock angles (upper panel) and cone angle (lower panel) for the events studied. The velocity deviation is obtained by subtracting the velocity for outward/sunward moving flux tube from the one for inward/earthward in a wave cycle. Positive (negative) ΔV represents outward/sunward (inward/earthward) motion. The open circles are for what have been observed in 2 April 2002.

reconnection. They stated that they could not resolve the speed of the magnetopause using measurements from the two spacecraft available at the time because of the small separation and inadequate CIS time resolution. In this study we estimate the motion of the magnetopause based on the direct correlation of solar wind dynamic pressure and local flow speed just inside the magnetopause during prolonged intervals when flow bursts were not present. Thus we provide a good reference frame for assessing flow speeds relative to the magnetopause.

[18] Budgeting ion mass flux in regions of source and transition in the magnetosphere provides basic information about the life cycle of the magnetospheric plasma of primary origins: solar wind (heliogenic) and ionosphere (geogenic). *Freeman* [1977] estimated the sunward convection of $\sim 10^8$ ions cm^{-2} s^{-1} using data from Geosynchronous satellite. *Heikkila* [1975] estimated the flux impinging on a merging area at the magnetopause of $\sim 5\ R_E^2$ and yielded $\sim 10^{27}$ ions s^{-1}. *Elphic et al.* [1997] applied the model of *Rasmussen et al.* [1993] and estimated the particle fluxes at geosynchronous orbits of 10^{26} ions s^{-1} at high latitudes ($\geq 25°$ to north and south) and 2.7×10^{26} at low latitudes ($<25°$ north and south) assuming an area of 15° in longitude and down to 2 R_E in altitude along the field lines. Ionospheric ion outflow was estimated by *Chappell et al.* [1987] and *Moore et al.* [1999] at $\sim 10^8$ ions cm^{-2} s^{-1} (quiet time) to 10^{10} ions cm^{-2} s^{-1} (high geomagnetic activities). The rate of ion outflow is $\sim 10^{25}$ ions s^{-1} during quiet time and above $\sim 10^{26}$ ions s^{-1} during high geomagnetic activities, and interestingly the rates of plasma sheet particle loss to the auroral zone falls between 10^{25} and 10^{26} ions s^{-1} [*Hill*, 1974; *Pilipp and Morfill*, 1976]. Table 5 summarizes the gain and lost of plasma in the dayside magnetosphere.

[19] Reconnection rate in MHD theory is defined by the Alfvén Mach number M_A [*Sweet*, 1958; *Parker*, 1963]: the ratio of velocity component normal to the magnetopause and the local Alfvén speed in the inflow region. The flow bursts observed are at the speeds of ~ 100 km s^{-1} relative to boundary oscillations or ~ 0.3 local M_A perpendicular to the magnetic field. This implies a reconnection rate of the same magnitude. Such rates exceed the estimates by *Petschek* [1964] and *Sonnerup* [1979] or the *Priest and Forbes* [1986] rapid reconnection model, which are on the order of 0.1. Although no shocks were identified besides the changing in the orientation of the magnetic field when flow bursts were encountered, ambiguities exist in where the flow bursts were located within the pictures of reconnection models that include inhomogeneity in the inflow region upstream of the shock boundary. Further complexity is added when multiple reconnection sites occur in the presence of a finite B_y component in the magnetosheath [*Luhmann et al.*, 1984; *Schindler et al.*, 1988; *Crooker et al.*, 1990; *Lee et al.*, 1993; *Moore et al.*, 2002] as observed in most of our cases. We cannot determine from this study whether there is a single X-line or multiple X-line segments extending over a wide range of latitudes and longitudes on the magnetopause.

4. Conclusions

[20] We have reported a substantial number of events of fast flows of relatively cold plasma flowing toward the magnetopause, as observed from the Polar spacecraft when it was near but inside the low latitude magnetopause during its recent skimming orbit phase. The ob-

Table 5. Ion Flux Estimates From Various Studies in Various Locations in the Magnetosphere

	Gain From Ionosphere, ions s^{-1}	Convect Toward Magnetopause, ions s^{-1}	Merge Into LLBL, ions s^{-1}[a]	Enter LLBL From Solar Wind, ions s^{-1}[b]
Chappell et al. (Polar Wind, OGO-5)	$1.5–5 \times 10^{26}$			
Moore et al. (Ion outflows, POLAR)	$10^{25}–10^{26}$			
Freeman (Plasmasphere, GEOS)		10^{27}		
Elphic et al. (Plasmasphere, GEOS)		2.7×10^{26}		
Chappell et al. (Plasma trough, OGO-5)		$3 \times 10^{25}–1.3 \times 10^{26}$		
This study (Magnetopause, POLAR)			$4 \times 10^{25}–2 \times 10^{27}$[a]	
Heikkila (model)				8×10^{26}[b]

[a]Per 10 R_E^2: 1 R_E in width by 10 R_E in length in latitudinal cross section of a flux tube along the magnetopause.
[b]Assuming $n_{sw} \sim 5$ cm^{-3}, $v_{sw} \sim 400$ km s^{-1}, $B_{IMF} \sim 5$ nT, $A_{incident} \sim 10\ R_E^2$.

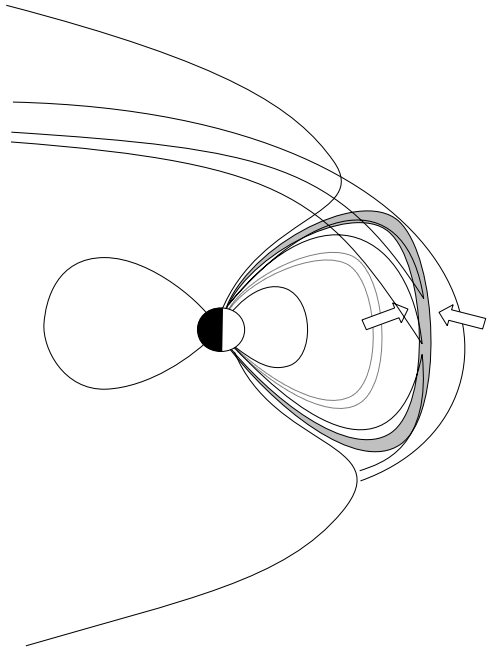

Figure 15. Schematic of reconnection at the dayside when IMF is southward and has a finite dawn-dusk component. We propose that the flow bursts Polar observed are the plasmas frozen in the reconnected and accelerated flux tube swept over high latitude magnetopause to the nightside.

served flowing plasmas have parameters characteristic of plasmaspheric plasma in the process of being convected to the dayside subsolar magnetopause region. The fast flows reported here appear to be related to southward IMF conditions, under relatively steady solar wind conditions, with few exceptions. They are accompanied by rotations of the local magnetic field away from the northward orientation typical of the magnetospheric boundary layer region. We therefore interpret them as the result of low latitude reconnection occurring in the subsolar region, drawing internal magnetospheric plasma to the boundary layer as plasma flux tubes are peeled away. Figure 15 shows a schematic of reconnection at the dayside when IMF is southward and has a finite dawn-dusk component. We propose that the flow bursts Polar observed are the plasmas frozen in flux tubes about to be reconnected and accelerated over the high latitude magnetopause to the night side. The particle fluxes carried by the flow bursts are comparable with that entering the reconnection region from the solar wind. We suggest that the plasma flow bursts supply a dynamically significant cold plasma to physical processes in the dayside boundary layers, including magnetic reconnection and related plasma instabilities.

[21] **Acknowledgments.** This work was supported by the Polar Mission under UPN 370-08-43 and by the NASA Office of Space Science Sun Earth Connection theme Research and Analysis program under UPN 432-01-42. We thank C. T. Russell at UCLA for providing magnetic field data, D. J. McComas at Southwest Research Institute, and N. F. Ness at Bartol Research Institute for making ACE solar wind and magnetic field data available through CDAWeb at NSSDC of NASA GSFC, and Peggy Sloan and Mike Chandler at NASA Marshall Space Flight Center for assistance with the TIDE software.

[22] Lou-Chuang Lee thanks James L. Horwitz for the assistance in evaluating this paper.

References

Barfield, J. N., and R. L. McPherron (1972), Investigation of interaction between Pc 1 and Pc 5 micropulsations at the synchronous orbit during magnetic storms, *J. Geophys. Res.*, *77*, 4707.

Borovsky, J. E., M. F. Thomsen, and D. J. McComas (1997), The superdense plasma sheet: Plasmaspheric origin, solar wind origin, or ionospheric origin?, *J. Geophys. Res.*, *102*, 22,089.

Brice, N. M. (1970), Artificial enhancement of energetic particle precipitation through cold plasma injection: A technique for seeding substorms?, *J. Geophys. Res.*, *75*, 4890.

Chandler, M. O., and T. E. Moore (2003), Observations of the geopause at the equatorial magnetopause: Density and temperature, *Geophys. Res. Lett.*, *30*(16), 1869, doi:10.1029/2003GL017611.

Chappell, C. R. (1974), Detached plasma regions in the magnetosphere, *J. Geophys. Res.*, *79*, 1861.

Chappell, C. R., K. K. Harris, and G. W. Sharp (1970), Study of the influence of magnetic activity on the location of the plasmapause as measured by OGO5, *J. Geophys. Res.*, *75*, 50.

Chappell, C. R., T. E. Moore, and J. H. Waite Jr. (1987), The ionosphere as a fully adequate source of plasma for the Earth's magnetosphere, *J. Geophys. Res.*, *92*, 5896–5910.

Crooker, N. U., G. L. Siscoe, and F. R. Toffoletto (1990), A tangent subsolar merging line, *J. Geophys. Res.*, *95*, 3787–3793.

Elphic, R. C., L. A. Weiss, M. F. Thomsen, D. J. McComas, and M. B. Moldwin (1996), Evolution of plasmaspheric ions at geosynchronous orbit during times of high geomagnetic activity, *Geophys. Res. Lett.*, *23*, 2189.

Elphic, R. C., M. F. Thomsen, and J. E. Borovsky (1997), The fate of the outer plasmasphere, *Geophys. Res. Lett.*, *24*, 365.

Engebretson, M. J., W. K. Peterson, J. L. Posch, M. R. Klatt, B. J. Anderson, C. T. Russell, H. J. Singer, R. L. Arnoldy, and H. Fukunishi (2002), Observations of two types of Pc 1–2 pulsations in the outer dayside magnetosphere, *J. Geophys. Res.*, *107*(A12), 1451, doi:10.1029/2001JA000198.

Freeman, J. W., H. K. Hills, T. W. Hill, P. H. Reiff, and D. A. Hardy (1977), Heavy ion circulation in the Earth's magnetosphere, *Geophys. Res. Lett.*, *4*, 195.

Fuselier, S. A. (1995), Kinetic aspects of reconnection at the magnetopause, in *Physics of the Magnetopause*, *Geophys. Monogr. Ser.*, vol. 90, edited by P. Song, B. U. Ö. Sonnerup, and M. F. Thomsen, pp. 181–188, AGU, Washington D. C.

Fuselier, S. A., D. M. Klumpar, W. K. Peterson, and E. G. Shelley (1989), Direct injection of ionospheric O^+ into the dayside low latitude boundary layer, *Geophys. Res. Lett.*, *16*, 1121.

Fuselier, S. A., D. M. Klumpar, and E. G. Shelley (1991), Ion reflection and transmission during reconnection at the Earth's subsolar magnetopause, *Geophys. Res. Lett.*, *18*, 139.

Fuselier, S. A., B. J. Anderson, and T. G. Onsager (1995), Particle signatures of magnetic topology at the magnetopause: AMPTE/CCE observations, *J. Geophys. Res.*, *100*, 11,805.

Gosling, J. T., M. F. Thomsen, S. J. Bame, R. C. Elphic, and C. T. Russell (1990), Cold ion beams in the low-latitude boundary layer during accelerated flow events, *Geophys. Res. Lett.*, *17*, 2245.

Grebowsky, J. M. (1970), Model study of plasmapause motion, *J. Geophys. Res.*, *75*, 4329.

Grebowsky, J. M., Y. Tulunay, and A. J. Chen (1973), Temporal variations in the dawn and dusk midlatitude trough position-Modeled and measured (Ariel 3), *NASA-GSFC Doc. X-621-73-149*, NASA Goddard Space Flight Cent., Greenbelt, Md.

Heikkila, W. J. (1975), Is there an electrostatic field tangential to the dayside magnetopause and neutral line?, *Geophys. Res. Lett.*, *2*, 154.

Hill, T. W. (1974), Origin of the plasma sheet, *Rev. Geophys.*, *12*, 379.

Horwitz, J. L., R. H. Comfort, and C. R. Chappell (1990), A statistical characterization of plasmasphere density structure and boundary locations, *J. Geophys. Res.*, *95*, 7937.

Kivelson, M. G., and G. T. Russell (1973), Active experiments, magnetospheric modification, and a naturally occurring analogue, *Radio Sci.*, *8*, 1035.

Lee, L. C., Z. W. Ma, Z. F. Fu, and A. Otto (1993), Topology of magnetic flux ropes and formation of fossil flux transfer events and boundary layer plasmas, *J. Geophys. Res.*, *98*, 3943.

Luhmann, J. G., R. J. Walker, C. T. Russell, N. U. Crooker, J. R. Spreiter, and S. S. Stahara (1984), Patterns of potential magnetic field merging sites on the dayside magnetopause, *J. Geophys. Res.*, *89*, 1739.

Maynard, N. C., and A. J. Chen (1975), Isolated cold plasma regions: Observations and their relation to possible production mechanisms, *J. Geophys. Res.*, *80*, 1009.

Moldwin, M. B., M. F. Thomsen, S. J. Bame, D. J. McComas, and G. D. Reeves (1995), The fine-scale structure of the outer plasmasphere, *J. Geophys. Res.*, *100*, 8021.

Moore, T. E., et al. (1995), The Thermal Ion Dynamics Experiment and Plasma Source Instrument, *Space Sci. Rev.*, *71*, 409.

Moore, T. E., R. Lundin, D. Alcayde, M. Andre, S. B. Ganguli, M. Temerin, and A. Yau (1999), Source processes in the high-latitude ionosphere, *Space Sci. Rev.*, *88*, 7.

Moore, T. E., M.-C. Fok, and M. O. Chandler (2002), The dayside reconnection X line, *J. Geophys. Res.*, *107*(A10), 1332, doi:10.1029/2002JA009381.

Mozer, F. S., S. D. Bale, and T. D. Phan (2002), Evidence of diffusion regions at a subsolar magnetopause crossing, *Phys. Rev. Lett*, *89*, 015002.

Parker, E. N. (1963), The solar-flare phenomenon and the theory of reconnection and annihilation of magnetic fields, *Astrophys. J., Suppl. Ser.*, *8*, 177.

Peterson, W. K., E. G. Shelley, G. Haerendel, and G. Paschmann (1982), Energetic ion composition in the subsolar magnetopause and boundary layer, *J. Geophys. Res.*, *87*, 2139.

Petschek, H. E. (1964), Magnetic field annihilation, in *AAS-NASA Symposium on the Physics of Solar Flares*, edited by W. N. Hess, *NASA Spec. Publ.*, *SP-50*, 425.

Pilipp, W., and G. Morfill (1976), The plasma mantle as the origin of the plasma sheet, in *Magnetospheric Particles and Fields*, edited by B. M. McCormac, p. 55, D. Reidel, Norwell, Mass.

Priest, E. R., and T. G. Forbes (1986), New models for fast steady state magnetic reconnection, *J. Geophys. Res.*, *91*, 5579.

Rasmussen, C. E., S. M. Guiter, and S. G. Thomas (1993), Two-dimensional model of the plasmasphere: Refilling time constants, *Planet. Space Sci.*, *41*, 35–43.

Rowland, D. E., and J. R. Wygant (1998), Dependence of the large-scale, inner magnetospheric electric field on geomagnetic activity, *J. Geophys. Res.*, *103*, 14,959.

Russell, C. T., R. C. Snare, J. D. Means, D. Pierce, D. Dearborn, M. Larson, G. Barr, and G. Le (1995), The GGS/Polar magnetic fields investigation, in *The Global Geospace Mission*, edited by C. T. Russell, p. 563, Kluwer Acad., Norwell, Mass.

Sandel, B. R., R. A. King, W. T. Forrester, D. L. Gallagher, A. L. Broadfoot, and C. C. Curtis (2001), Initial results from the IMAGE Extreme Ultraviolet Imager, *Geophys. Res. Lett.*, *28*(8), 1439, doi:10.1029/2001GL012885.

Sauvaud, J.-A., et al. (2001), Intermittent thermal plasma acceleration linked to sporadic motions of the magnetopause, first Cluster results, *Ann. Geophys.*, *19*, 1523–1532.

Schindler, K., M. Hesse, and J. Birn (1988), General magnetic reconnection, parallel electric fields, and helicity, *J. Geophys. Res.*, *93*, 5547.

Seki, K., R. C. Elphic, M. F. Thomsen, J. Bonnell, J. P. McFadden, E. J. Lund, M. Hirahara, T. Terasawa, and T. Mukai (2002), A new perspective on plasma supply mechanisms to the magnetotail from a statistical comparison of dayside mirroring O^+ at low altitudes with lobe/mantle beams, *J. Geophys. Res.*, *107*(A4), 1047, doi:10.1029/2001JA900122.

Shue, J.-H., J. K. Chao, H. C. Fu, C. T. Russell, P. Song, K. K. Khurana, and H. J. Singer (1997), A new functional form to study the solar wind control of the magnetopause size and shape, *J. Geophys. Res.*, *102*, 9497.

Singer, H. J., D. J. Southwood, R. J. Walker, and M. G. Kivelson (1981), Alfvén wave resonances in a realistic magnetospheric magnetic field geometry, *J. Geophys. Res.*, *86*, 4589–4596.

Sonnerup, B. U. Ö. (1979), Magnetic field reconnection, in *Solar System Plasma Physics*, vol. 3, edited by by C. F. Kennel, L. T. Lanzerotti, and E. N. Parker, p. 45, North-Holland, New York.

Su, Y.-J., J. E. Borovsky, M. F. Thomsen, R. C. Elphic, and D. J. McComas (2000), Plasmaspheric material at the reconnecting magnetopause, *J. Geophys. Res.*, *105*, 7591.

Su, Y.-J., J. E. Borovsky, M. F. Thomsen, N. Dubouloz, M. O. Chandler, T. E. Moore, and M. Bouhram (2001), Plasmaspheric material on high-latitude open field lines, *J. Geophys. Res.*, *106*, 6085.

Summers, D., and R. M. Thorne (2003), Relativistic electron pitch-angle scattering by electromagnetic ion cyclotron waves during geomagnetic storms, *J. Geophys. Res.*, *108*(A4), 1143, doi:10.1029/2002JA009489.

Sweet, P. A. (1958), The neutral point theory of solar flares, in *Electromagnetic Phenomena in Cosmical Physics*, edited by B. Lehnert, p. 135, Cambridge Univ. Press, New York.

Takahashi, K., R. E. Denton, and D. Gallagher (2002), Toroidal wave frequency at L = 6–10: Active Magnetospheric Particle Tracer Explorers/CCE observations and comparison with theoretical model, *J. Geophys. Res.*, *107*(A2), 1020, doi:10.1029/2001JA000197.

Taylor, H. A., J. M. Grebowsky, and W. J. Walsh (1971), Structured variations of the plasmapause: Evidence of a corotating plasma tail, *J. Geophys. Res.*, *76*, 6806.

Thorne, R. M. (1974), A possible cause of dayside relativistic electron precipitation events, *J. Atmos. Terr. Phys.*, *36*, 635.

S.-H. Chen and T. E. Moore, NASA Goddard Space Flight Center, Code 692, Greenbelt, MD 20771, USA. (sheng-hsien.chen@gsfc.nasa.gov; thomas.e.moore@gsfc.nasa.gov)